CHEMISTRY
A EUROPEAN JOURNAL

DOI: 10.1002/chem.201000185

Anilinic N-Oxides Support Cytochrome P450-Mediated N-Dealkylation through Hydrogen-Atom Transfer

Kenneth M. Roberts and Jeffery P. Jones*[a]

Abstract: The mechanism of N-dealkylation mediated by cytochrome P450 (P450) has long been studied and argued as either a single electron transfer (SET) or a hydrogen atom transfer (HAT) from the amine to the oxidant of the P450, the reputed iron–oxene. In our study, tertiary anilinic N-oxides were used as oxygen surrogates to directly generate a P450-mediated oxidant that is capable of N-dealkylating the dimethylaniline derived from oxygen donation. These surrogates were employed to probe the generated reactive oxygen species and the subsequent mechanism of N-dealkylation to distinguish between the HAT and SET mechanisms. In addition to the expected N-demethylation of the product aniline, 2,3,4,5,6-pentafluoro-*N*,*N*-dimethylaniline *N*-oxide (PFDMAO) was found to be capable of N-dealkylating both *N*,*N*-dimethylaniline (DMA) and *N*-cyclopropyl-*N*-methylaniline (CPMA). Rate comparisons of the N-demethylation of DMA supported by PFDMAO show a 27-fold faster rate than when supported by *N*,*N*-dimethylaniline *N*-oxide (DMAO). Whereas intermolecular kinetic isotope effects were masked, intramolecular measurements showed values reflective of those seen previously in DMAO- and the native NADPH/O_2-supported systems (2.33 and 2.8 for the N-demethylation of PFDMA and DMA from the PFDMAO system, respectively). PFDMAO-supported N-dealkylation of CPMA led to the ring-intact product *N*-cyclopropylaniline (CPA), similar to that seen with the native system. The formation of CPA argues against a SET mechanism in favor of a P450-like HAT mechanism. We suggest that the similarity of KIEs, in addition to the formation of the ring-intact CPA, argues for a similar mechanism of Compound I (Cpd I) formation followed by HAT for N-dealkylation by the native and N-oxide-supported systems and demonstrate the ability of the N-oxide-generated oxidant to act as an accurate mimic of the native P450 oxidant.

Keywords: cytochromes · hydrogen transfer · iron · N-dealkylation · N-oxides

Introduction

Cytochrome P450 (P450) enzymes are a ubiquitous superfamily of heme-containing monoxygenases capable of oxidizing endogenous and exogenous substrates, including the majority of clinically relevant pharmaceuticals.[1] Decades of study have been spent understanding the mechanism of P450-mediated oxidation. The consensus mechanism involves a multistep activation of molecular oxygen.[1] Activation leads to a series of oxygen intermediates that culminate in an iron(IV)–oxo porphyrin π-radical cation similar to the Compound I (Cpd I) species of chloroperoxidase as the reactive oxygen species (ROS) in these reactions.[1–4]

N-Dealkylation has been studied as one of the many oxidations performed by the proposed Cpd I. The pathway involves oxygen insertion by Cpd I into the C_α–H bond to generate a carbinolamine that spontaneously dealkylates forming the free amine and aldehyde (Scheme 1). Recent

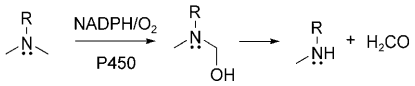

Scheme 1. N-Dealkylation (N-demethylation) overview.

studies of this pathway have centered on two proposed mechanisms.[5] One mechanism proposes a single electron transfer (SET) from the target nitrogen to Cpd I forming an iron(IV)–oxo porphyrin (Cpd II) and an aminium radical cation (Scheme 2). Cation formation increases the acidity of

[a] Dr. K. M. Roberts, Prof. J. P. Jones
Department of Chemistry, Washington State University
PO BOX 644630, Pullman, WA 99164-4630 (USA)
Fax: (+1) 509-335-8867
E-mail: jpj@wsu.edu

Supporting information for this article is available on the WWW under http://dx.doi.org/10.1002/chem.201000185.

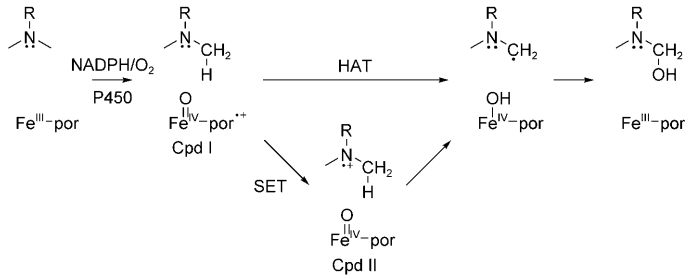

Scheme 2. Pathways for hydrogen atom transfer (HAT) and single electron transfer (SET) (por = porphyrin).

C_α and drives a subsequent proton transfer to Cpd II. The final step is the barrierless formation of the carbinolamine by transfer of a hydroxyl radical to the resulting carbon radical.[6] In contrast, the second mechanism proposes that Cpd I elicits a hydrogen atom transfer (HAT) from C_α to directly form the carbon radical and the protonated Cpd II (Scheme 2). In attempts to distinguish between SET and HAT mechanisms in metal-catalyzed N-dealkylations, studies with biomimetic systems have argued for SET mechanisms in these systems.[7–10] Addressing this issue in enzymatic systems, Shaffer et al. introduced *N*-cyclopropyl-*N*-methylaniline (CPMA) as a new probe for distinguishing between the two mechanisms.[11,12] They found that P450-mediated oxidation of CPMA led to products that left the cyclopropyl ring intact.[12] This was in contrast to the solely ring-open products found upon oxidation by horseradish peroxidase (HRP),[11] an enzyme known to undergo a SET mechanism.[13,14] They concluded that P450 follows a HAT mechanism in the exclusion of the SET mechanism. Further, Cerny and Hanzlik found that P450-mediated oxidation of tertiary cyclopropylamines led to both ring-intact and ring-open products.[15] However, ring-open products only appeared in the second round of N-dealkylation. Simply, a prior round of N-dealkylation was required and ring-opened products derived solely from the ring-intact secondary amine product of the first N-dealkylation. They concluded a HAT mechanism for N-dealkylation that incorporated abstraction of the N hydrogen as explanation of the ring-open products.

Confirmation of the HAT mechanism, as well as other oxidations proposed to act via Cpd I, requires showing that Cpd I elicits these reactions. However, the activation of molecular oxygen leading to Cpd I is complex and involves several steps including proton and electron transfers.[1] Due to this complicated process, alternate sources of generating this species directly for use as mechanistic probes have been explored. These compounds, termed oxygen surrogates, include iodosylbenzene (PhIO), cumene hydroperoxide (CuOOH), and substituted *N*,*N*-dimethylaniline *N*-oxides (DMAOs). Yet, the ROSs resulting from surrogacy have recently come into question as valid mimics of P450 Cpd I.[4,16,17] Studies by Dawson et al. observing Cpd I formation by oxygen surrogates found no evidence for Cpd I when P450BM3 was exposed to PhIO.[4] Bichara et al. compared propranolol oxidation in P4502D6 supported by CuOOH and the native NADPH/O_2 system and found different preferences for sites of oxidation for the two oxidants.[18] Further, Guengerich et al. showed that the kinetic isotope effects (KIEs) of the N-dealkylation of two substituted *N*,*N*-dimethylanilines (DMAs) by PhIO and CuOOH were large (6.7–7.3 and 3.4–3.7, respectively) compared to the small KIEs (1.7–2.3) seen for the native NADPH/O_2 pathway of the enzyme.[16] This difference was supported by theoretical calculations from Shaik's group, who concluded that PhIO and NADPH/O_2 generated unique spin states of Cpd I and that these spin states were responsible for the different isotope effects.[17]

In contrast, anilinic N-oxides, such as *N*,*N*-dimethylaniline *N*-oxide, have recently been shown to generate an oxidant that strongly mimics the oxidant of the NADPH/O_2 pathway. Dowers et al., compared the KIEs of the N-demethylation of substituted DMAs by their respective N-oxides and by NADPH/O_2 and found them to be identical.[19] It was hypothesized that DMAOs donate a six-electron oxygen (oxene) directly generating Cpd I, which in turn oxidizes the resulting DMA (Scheme 3 A).

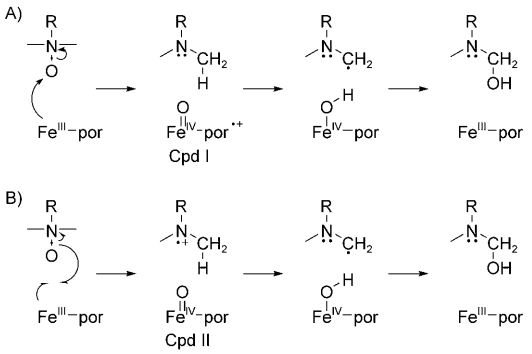

Scheme 3. Proposed formations of Cpd I (A) and Cpd II (B) by oxygen donation from an N-oxide (por = porphyrin).

Theoretical calculations by Shaik's group supported this conclusion finding that oxygen donation by DMAO generates Cpd I with a calculated energy barrier of 21 kcal mol^{-1}.[17] In comparison, for the N-demethylation step, they calculated Cpd I spin-state-dependent energy barriers of 6.4 kcal mol^{-1} and 8.8 kcal mol^{-1} for the doublet and quartet, respectively, demonstrating the rate-determining nature of the oxygen donation.

DMAO-generated Cpd I would be expected to support oxidation of secondary substrates. However, in early work with a porphyrin mimetic system, Bruice and Nee found DMAO unable to significantly support olefin epoxidation.[20] They rationalized that the ease of oxidation of DMA outcompeted olefin epoxidation for the putative iron–oxene (Cpd I) and that increasing the oxygen donation rate and decreasing the rate of N-dealkylation would be required to facilitate oxygen surrogacy. They proposed that electron-withdrawing substituents on the aromatic ring would realize

both effects and, in support of this, they successfully tested *p*-cyano-*N*,*N*-dimethylaniline *N*-oxide (CDMAO) as a surrogate oxygen donor able to support various olefin epoxidations as well as cyclohexane hydroxylation.[20]

In a study with P4502B1, however, Seto and Guengerich found that they were unable to significantly oxidize a second distinct DMA with either DMAO or CDMAO.[21] They concluded that oxygen donation resulted from homolytic cleavage of the N–O bond generating Cpd II and the aminium radical cation (Scheme 3B). While Cpd II is poised to deprotonate the C_α of the aminium radical, the oxidant would not be electrophilic enough to react with an unoxidized DMA.

In this work, we investigated the nature of the ROS generated by anilinic N-oxides in P450 and its ability to oxidize secondary substrates. With a P450 HAT mechanism for N-dealkylation supported by the work of Shaffer et al. with CPMA[12] and the identical KIE values found by Dowers et al. for N-dealkylation by DMAOs and P450,[19] we hypothesized that DMAOs donate an oxene to the P450 heme to form a Cpd I poised to oxidize the resulting DMA through a HAT mechanism. Further, similar to Bruice and Nee,[20] we proposed that DMAO surrogacy is limited by the ease of oxidation of the subsequent DMA and that increasing the electron-withdrawing character on the aromatic ring would increase the rate of oxygen donation and slow down the N-demethylation of the subsequent aniline. To evaluate these considerations, we employed a newly synthesized oxygen surrogate, 2,3,4,5,6-pentafluoro-*N*,*N*-dimethylaniline *N*-oxide (PFDMAO), with the expectation that the heavily electron-withdrawing fluorines would increase the rate of Cpd I formation and decrease the rate of N-dealkylation, unmasking its ability to act as a surrogate. Experimental results demonstrate that oxygen donation by PFDMAO is faster than by DMAO with support by theoretical calculations that show a lower barrier. We also show that the PFDMAO-derived oxidant is capable of N-dealkylating DMA and CPMA, substrates distinct from the generated aniline. In the surrogate system, N-demethylation of DMA is faster than that of the resulting 2,3,4,5,6-pentafluoro-*N*,*N*-dimethylaniline (PFDMA), supporting the greater ease of oxidation of DMA relative to the more electron-withdrawn PFDMA. Further, N-dealkylation of CPMA formed the ring-intact product *N*-cyclopropylaniline (CPA). CPA formation, kinetic values and theoretical calculations support a mechanism of Cpd I formation followed by HAT.

Results and Discussion

Oxygen donation rates: A number of questions remain about the mechanism of oxygen donation by anilinic N-oxides, including the rate-determining step of the pathway, the nature of the oxidant formed and the consequent chemistry of N-dealkylation. We first address the rate-determining step in the N-oxide pathway. Scheme 4 demonstrates a simple mechanism of N-oxide binding, oxygen transfer,

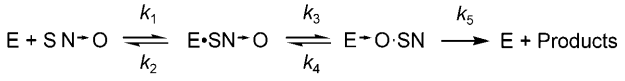

Scheme 4. Kinetic scheme for oxygen donation.

and product formation. As described above, the calculations of DMAO by Shaik's group show a much higher barrier to oxygen donation (k_3) than oxidation of the aniline (k_5), 21 kcal mol^{-1} and 6.4–8.8 kcal mol^{-1}, respectively. This higher barrier supports oxygen donation as the rate-determining step in this pathway.[17] We examined the rate-determining step experimentally by using KIEs for the N-demethylation of an N-oxide by P450cam. Product formation rates for *p*-cyano-*N*,*N*-dimethylaniline *N*-oxide (CDMAO) and *p*-cyano-*N*,*N*-bis(trideuteriomethyl)aniline *N*-oxide ([D_6]CDMAO) were compared in intermolecular experiments. Kinetic isotope effects were calculated from the ratios of *p*-cyano-*N*-methylaniline and *p*-cyano-*N*-(trideuteriomethyl)aniline formed, both in separate incubations (noncompetitive) and when incubated together (competitive). Given Scheme 4, three possibilities for isotope effects are expected that depend on the rate-determining step: 1) On-rates (k_{1H}/k_{1D}) would be expected to display no isotope effect, so if binding is rate-determining, no isotope effect on product formation would be observed; 2) a rate-determining oxygen donation (k_{3H}/k_{3D}) would show a β-secondary isotope effect on product formation; β-secondary isotope effects, however, can be small and may be indistinguishable from 1. 3) If N-demethylation (k_{5H}/k_{5D}) is rate-determining, a KIE of around 2.8 would be expected based on intrinsic isotope effect values measured experimentally by Dower et al.[19] Our intermolecular experiments show no significant isotope effect (Table 1). This suggests that the isotope effect

Table 1. Kinetic isotope effects on N-demethylation by N-oxide-supported P450cam.

	k_H/k_D—[D_0]/[D_6] noncompetitive[a,b]	k_H/k_D—[D_0]/[D_6] competitive[a,b]	k_H/k_D intramolecular
CDMAO[c]	0.9 ± 0.2	1.2 ± 0.1	2.77 ± 0.05[e]
PFDMAO[d]	1.2 ± 0.2	1.3 ± 0.2	2.33 ± 0.07[f]

[a] [D_0] = unlabeled. [b] [D_6] = (CD_3)$_2$-labeled. [c] CDMAO = *p*-cyano-*N*,*N*-dimethylaniline *N*-oxide. [d] PFDMAO = 2,3,4,5,6-pentafluoro-*N*,*N*-dimethylaniline *N*-oxide. [e] From reference [19]. [f] Measured by using 2,3,4,5,6-pentafluoro-*N*-methyl-*N*-trideuteriomethylaniline

for N-dealkylation is being masked by a prior, slower step: either substrate binding or oxygen donation. Surface plasmon resonance measurements by Pearson et al. of the binding of the rod-like antifungals itraconazole and ketoconazole with P450 3A4 measured substrate on-rates of 10^3–10^4 M^{-1} s^{-1}, much faster than either substrate or product off-rates.[22] That the non-globular substrates itraconazole and ketoconazole can still bind enzyme at this rate demonstrates the rapidity of substrate binding, excluding binding as the rate-determining step. The exclusion of the steps of sub-

strate binding and N-dealkylation supports oxygen donation as rate-determining with CDMAO.

As a consequence of the electron-withdrawing character of the *p*-cyano group, Bruice and Nee had used CDMAO to increase the rate of oxygen donation relative to DMAO in their experiments.[20] In an effort to further increase the rate of oxygen donation, we turned to 2,3,4,5,6-pentafluoro-*N*,*N*-dimethylaniline *N*-oxide (PFDMAO). The electron-withdrawing character of the fluorines was expected to further weaken the N–O bond and increase the rate of oxygen donation. We performed DFT calculations for oxygen donation by PFDMAO and found a barrier of 10.6 kcal mol^{-1} (Figure 1), significantly less than calculated by Cho et al. for

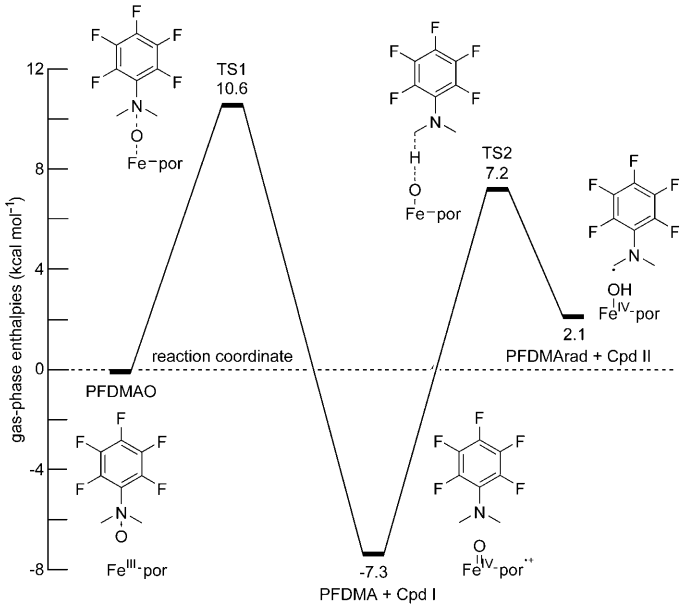

Figure 1. Energies calculated by density functional theory for the reaction of PFDMAO with P450. Values are uncorrected for zero-point energies or solvation effects. TS1 = transition state for oxygen donation; TS2 = transition state for hydrogen atom transfer; PFDMArad = PFDMA carbon-centered radical (por = porphyrin).

DMAO.[17] Further, the calculations support a barrier for N-demethylation of the product aniline (PFDMA) of 14.5 kcal mol^{-1}, several kcal mol^{-1} higher than that seen by Cho et al. for DMAO[17] and 4 kcal mol^{-1} larger than that for oxygen donation. This larger barrier implies that N-demethylation should be rate-determining in the PFDMAO system. Our calculations followed the reaction to the PFDMA carbon-centered radical (Figure 1). Whereas this portrays an endothermic reaction, Li et al. have demonstrated that oxygen rebound is barrierless in the DMAO reaction leading to very exothermic products (greater than 50 kcal mol^{-1}).[23] The products of oxygen rebound in the PFDMAO reaction are expected to be similarly exothermic.

In light of our calculations, PFDMAO was synthesized and kinetic isotope effects measured in P450cam to determine if this predicted faster oxygen donation resulted in a change of the rate-determining step, thus, unmasking the intrinsic isotope effect. Intramolecular isotope effects were determined by using 2,3,4,5,6-pentafluoro-*N*-methyl-*N*-trideuteriomethylaniline *N*-oxide ([D_3]PFDMAO) and measuring the ratio of 2,3,4,5,6-pentafluoro-*N*-methylaniline (PFMA) and 2,3,4,5,6-pentafluoro-*N*-trideuteriomethylaniline ([D_3]PFMA). Intermolecular isotope effects were determined by using PFDMAO and 2,3,4,5,6-pentafluoro-*N*,*N*-bis(trideuteriomethyl)aniline *N*-oxide ([D_6]PFDMAO) and measuring the ratios of the products PFMA and [D_3]PFMA, both in competitive and noncompetitive experiments. Whereas a significant intramolecular isotope effect was seen, no significant isotope effect for N-demethylation in both the noncompetitive and competitive experiments was observed (Table 1). As with CDMAO, the lack of an intermolecular isotope effect suggests that the intrinsic isotope effect is masked by a prior step in the PFDMAO system and that oxygen donation is still rate-determining. We expect that the disagreement between the DFT calculations and experimental results arises from the similarity of the calculated barrier heights for oxygen donation and N-dealkylation (10.6 and 14.5 kcal mol^{-1}). These values are not so dissimilar as to be distinguishable by DFT calculations.

Though isotope effects suggest no change in the rate-determining step for the PFDMAO system, it is still in question whether the barrier for this step has been lowered. PFDMAO and the unsubstituted DMAO were incubated with P450cam and product formation rates were measured. As shown in Table 2, the rate of N-demethylation from PFDMAO was 27-fold faster than that of DMAO. Further,

Table 2. Product formation rates by P450cam supported by DMAO or PFDMAO.

N-Oxide	Rate [nmol min^{-1} nmol P450^{-1}] Dimethyl product	Methyl product
DMAO[a]	0	1.2 ± 0.2
PFDMAO[b]	1.5 ± 0.3	32 ± 2

[a] DMAO = *N*,*N*-dimethylaniline *N*-oxide. [b] PFDMAO = 2,3,4,5,6-pentafluoro-*N*,*N*-dimethylaniline *N*-oxide.

the unoxidized 2,3,4,5,6-pentafluoro-*N*,*N*-dimethylaniline (PFDMA) was also isolated as a product. With N-demethylation expected to require the prior step of oxygen donation, combining the rates of both products in the PFDMAO system gives a total rate of product formation of 34 nmol min^{-1} nmol P450^{-1}, a rate 28-fold faster than for DMAO. Changes in the rate of product formation indicate a change in the rate-determining step. With isotope effects supporting oxygen donation as rate-determining, the increased rate of product formation suggests a lowering of the barrier to oxygen donation.

The faster rate of oxygen donation by PFDMAO also lends insight to the mechanism of oxygen donation. The electron-withdrawing nature of the aromatic fluorines offers two outcomes for rate effects on oxygen donation, dependent on the nature of the N–O bond scission. As discussed

above, two distinct oxygen donation mechanisms have been proposed for N-oxide systems, a six-electron oxygen (oxene) donation and a seven-electron oxygen donation. Donation of an oxene results from heterolytic cleavage of the N–O bond, which returns both electrons to the nitrogen of the aniline (Scheme 5). Electron-withdrawing groups would be

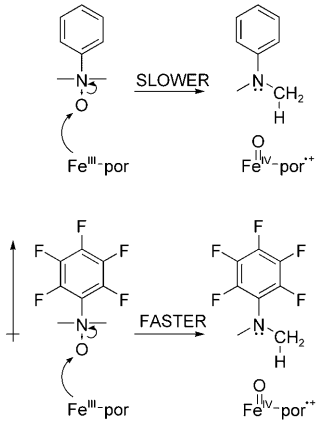

Scheme 5. Electronic effects on heterolytic cleavage of the N–O bond of DMAO and PFDMAO (por = porphyrin).

expected to pull the electrons away from the nitrogen and the N–O bond, weakening the latter. Oxygen donation and Cpd I formation from heterolytic cleavage would be expected to be faster as a result of the weakened bond. This is supported by the over 10 kcal mol^{-1} lower activation energy for oxygen donation from PFDMAO versus DMAO in DFT calculations (Figure 1 and reference [13]). In contrast, donation of a seven-electron oxygen requires homolytic cleavage of the N–O bond, forming an aminium radical and Cpd II (Scheme 6). Electron-withdrawing substituents would further increase the positive charge on the nitrogen in the aminium radical. Destabilization of the product would be expected to be reflected in a slower rate of oxygen donation. This is represented in the gas-phase energies of the aniline

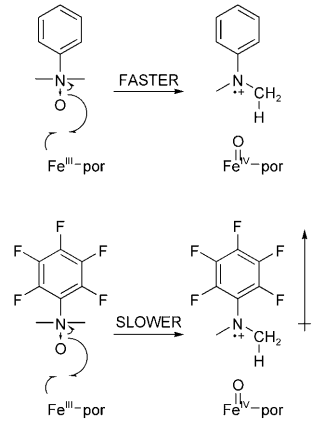

Scheme 6. Electronic effects on homolytic cleavage of the N–O bond of DMAO and PFDMAO (por = porphyrin).

radical cations relative to their neutral anilines as calculated by DFT: 282.32 and 154.76 kcal mol^{-1} for PFDMA and DMA, respectively. It is important to note that the destabilized aminium radical would be expected to show an increased acidity of the methyl proton and a faster rate of proton transfer. However, our isotope effect measurements demonstrate that breaking the C–H bond is not rate-determining and this increased rate would not be reflected in product formation rates. Since homolytic cleavage is expected to be slower with PFDMAO, the finding that PFDMAO donates its oxygen an order of magnitude faster than DMAO excludes donation of a seven-electron oxygen and the direct formation of Cpd II.

Further support for oxene donation is offered by spin density calculations on the products of oxygen donation. We used DFT calculations to observe the spin densities of the product of oxygen donation from DMAO and compared them to calculated spin densities of DMAO radical cation. As shown in Figure 2, the calculations show large spin densi-

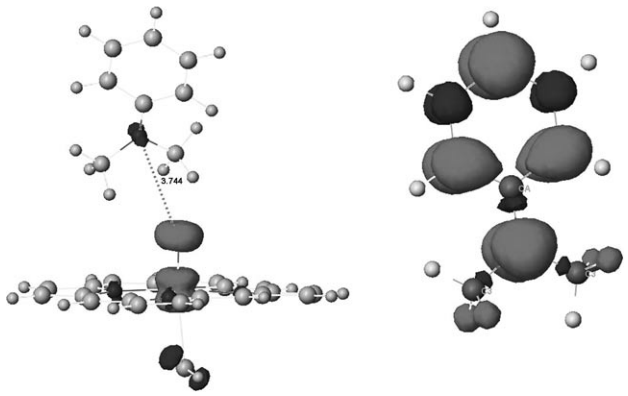

Figure 2. Calculated spin densities of the products of DMAO oxygen donation (left) and the DMA radical cation (right).

ty on the iron-centered oxygen with very little spin density on the anilinic nitrogen or the aromatic ring, indicative of a neutral aniline paired with Cpd I. In contrast, spin density calculations of an aminium radical cation show large spin density on the nitrogen and throughout the aromatic ring. We were unable to isolate Cpd II with the aminium radical. Instead, lengthening of the N–O bond generates Cpd I and the aniline. The evident differences between the spin densities for the donation products and an aniline radical cation further support the exclusion of homolytic cleavage of the N–O bond and direct Cpd II formation.

We have shown that the anilinic N-oxide-supported P450 pathway utilizes a mechanism that involves a fast N-dealkylation preceded by a rate-determining oxygen donation. However, though perfluorination of the aromatic ring did not result in a change in the rate-determining steps, product formation rates of the PFDMAO system were significantly increased compared to that of the unsubstituted DMAO system. These faster donation rates that result from the electron-withdrawing fluorines with support from DFT calcula-

tions exclude homolytic cleavage of the N–O bond to directly form Cpd II. In exclusion of the homolytic pathway, a mechanism that requires heterolytic cleavage of the N–O bond to form Cpd I is supported.

Oxygen surrogacy: Rate measurements and DFT calculations of the N-oxide-supported P450 system support a mechanism with a rate-determining oxene donation. With PFDMAO, this donation shows two fates for the product aniline (PFDMA): it is either N-demethylated or released from the enzyme (Table 2). The release of PFDMA requires oxene donation without the subsequent N-demethylation. With PFDMAO exhibiting faster rates for oxene donation and a small portion of the donated oxenes not participating in N-dealkylation, we tested the ability of PFDMAO to act as an oxygen surrogate. PFDMAO and P450cam were incubated in the presence of *N*,*N*-dimethylaniline (DMA) and *N*-cyclopropyl-*N*-methylaniline (CPMA). Both substrates were oxidized by P450cam when supported by PFDMAO with product formation rates shown in Table 3.

Table 3. Product formation rates from alternate substrates by PFDMAO-supported P450cam.

	Rate [nmol min^{-1} nmol P450^{-1}]			
	PFDMA[a]	PFMA[b]	MA[c]	CPA[d]
DMA[e]	63 ± 2	2.5 ± 0.1	33.0 ± 1	–
CPMA[f]	5 ± 1	3.7 ± 0.3	0.28 ± 0.03	0.6 ± 0.1

[a] PFDMA = 2,3,4,5,6-pentafluoro-*N*,*N*-dimethylaniline. [b] PFMA = 2,3,4,5,6-pentafluoro-*N*-methylaniline. [c] MA = *N*-methylaniline. [d] CPA = *N*-cyclopropylaniline. [e] DMA = *N*,*N*-dimethylaniline. [f] CPMA = *N*-cyclopropyl-*N*-methylaniline.

DMA was rapidly metabolized in the PFDMAO system with a rate of *N*-methylaniline (MA) formation 27-fold faster than the DMAO system. The rate of PFMA formation was decreased by a factor of ten, with the formation of MA 11-fold faster than that of PFMA. This is expected because the donated oxygen is given a choice of substrates. Any redirection of the oxygen towards DMA would result in a decrease in PFMA formation. Further, because DMA has a much lower oxidation potential, it is expected to outcompete PFDMA for the donated oxygen, as is seen. Expectedly, the rate of formation of PFDMA was increased in comparison to experiments without DMA. Redirection of the donated oxygen to the DMA prevents oxidation of PFDMA and, thus, permits its subsequent release. Total oxygen donation in the presence of DMA was doubled in comparison to experiments without DMA. Surprisingly, only half of the PFDMA formation is accounted for by N-demethylation products. The presence of DMA in the PFDMAO system appears to elicit a third pathway for the donated oxygen. We propose the formation of DMAO as this third pathway, though oxidation of the P450 active site is also a possibility.

Oxidation of CPMA in the PFDMAO system was much slower than either that of DMA or the system without substrate. CPMA was N-dealkylated to MA and *N*-cyclopropylaniline with a total rate of 0.9 nmol min^{-1} nmol P450^{-1}. N-Dealkylation of PFDMA was four times faster than that of CPMA. Total oxygen donation was about four-fold slower than the PFDMAO system without substrate and seven-fold slower than the PFDMAO system with DMA present. Having a methyl group replaced with a more electron-donating cyclopropyl group, CPMA should be more susceptible to oxidation than DMA and a higher rate of oxidation of CPMA would be expected. We expect the slower rates seen in the CPMA–PFDMAO system to be an active site binding effect, where CPMA inhibits PFDMAO from donating the oxygen. When PFDMAO is positioned for oxygen donation, the resulting PFDMA outcompetes the CPMA by a proximity effect. As with the DMA, total oxygen donation in the PFDMAO system with CPMA present is not fully accounted for by N-dealkylation products. In fact, approximately 80% of the PFDMA formation is unaccounted for. We expect that, like DMA, CPMA elicits a third pathway of N-oxygenation as the fate of the donated oxygen.

The ability of PFDMAO to significantly support oxidation of a second substrate is a feature previously unseen with DMAOs and P450. In the experiments with DMA, not only is the alternate substrate oxidized, but it outcompetes PFDMA, the product of oxene donation, for oxidation. The successful competition of DMA demonstrates the difficulty of the N-dealkylation of PFDMA. In the PFDMAO system, the more difficult oxidation of the product aniline (PFDMA) permits competition between oxidation and substrate exchange (Scheme 7). In contrast, the DMAO system does not allow competition for the oxidant, expectedly the result of the ease of oxidation of DMA. With the lifetime of Cpd I permitting substrate exchange in the PFDMAO system, the possibility of detection and characterization can be entertained, similar to work with other various oxygen surrogates by Dawson et al.[4] and Newcomb et al.[3,25] How-

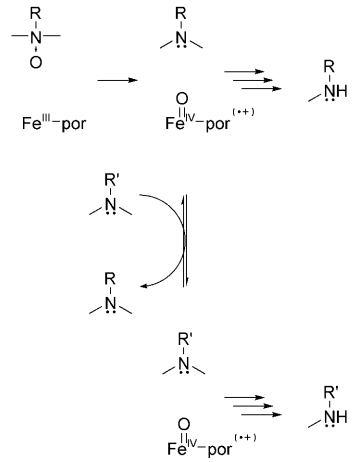

Scheme 7. Competition of *N*,*N*-dimethylanilines for an N-oxide-generated oxidant (por = porphyrin).

ever, no intermolecular isotope effects are observed with PFDMAO demonstrating the rate-determining nature of oxygen donation. There should be no significant buildup of the Cpd I intermediate making detection difficult or impossible.

The N-oxide-generated oxidant: PFDMAO has been found to be an oxene donor capable of acting as a surrogate for N-dealkylation. Product formation rates and DFT calculations support an oxene donation for anilinic N-oxides. However, what occurs downstream of Cpd I formation is unclear. With the observation that PFDMAO acts as an oxygen surrogate for other substrates and DMAO does not, three possible mechanisms for N-dealkylation in the N-oxide systems become apparent. Two are the SET and HAT mechanisms described above. The third mechanism is a SET-like pathway that involves an outer-sphere electron transfer between substrates.

In the HAT mechanism, after oxene donation by the N-oxide, the generated Cpd I abstracts a hydrogen from the C_α to form a carbon-centered radical (Scheme 8). The occurrence of competition for substrate oxidation is dependent on the relative rates of substrate oxidation and substrate exchange. The inability of DMAO to support the oxygenation of other compounds can be rationalized by its low barrier to oxidation that permits its oxidation before exchange with an alternate substrate can occur. Thus, when DMAO donates its oxygen to form Cpd I, the resulting DMA immediately transfers a hydrogen atom before any substrate exchange occurs. In contrast, hydrogen atom transfer from PFDMA is expected to be much slower. If substrate exchange is rapid compared to the oxidation of PFDMA, then the relative ease of oxidation presides over substrate preference. As described, DMA has a much lower barrier to single-electron oxidation than PFDMA. With its lower barrier to oxidation, DMA would be expected to be preferentially oxidized over PFDMA.

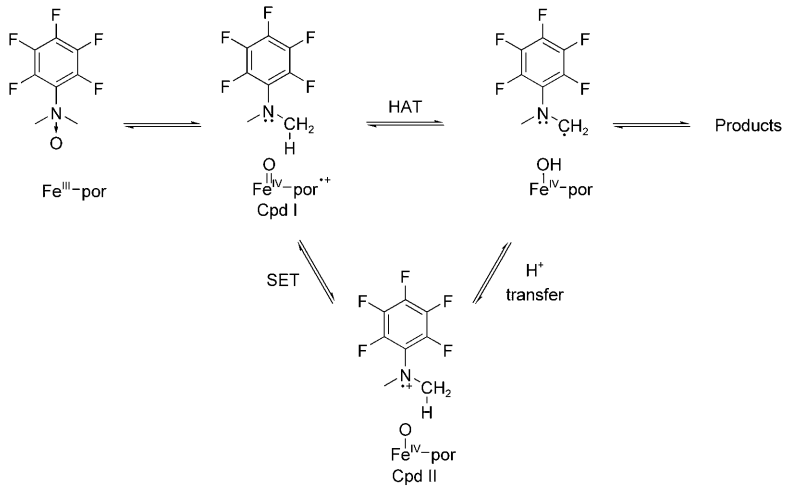

Scheme 8. Proposed N-oxide-supported HAT and SET mechanisms for N-dealkylation of PFDMAO (por = porphyrin).

In the basic SET pathway, after oxene donation to form Cpd I, a single electron transfer from the product aniline occurs to form an aminium radical cation and Cpd II (Scheme 8). Similar to the HAT mechanism, oxidation rates of substrates depend on the rate of substrate exchange and the ease of substrate oxidation. In the case of SET, the ease of oxidation is determined by the single-electron oxidation potential of competitive substrates. If substrate exchange is fast relative to the SET event, the substrate with the lowest oxidation potential will be oxidized first. With DMA having a lower barrier to oxidation than PFDMA (Figure 2), we would expect electron transfer from DMA to Cpd I to occur faster. However, with P450 2B1, Seto and Guengerich found only trace support of oxidation of [^{14}C]DMA by three distinct DMAOs, including the electron-withdrawn CDMAO, concluding that oxidation of a second substrate was prevented by a direct Cpd II formation from the N-oxide.[21] We have excluded the direct formation of Cpd II by showing a higher rate of oxygen donation by PFDMAO over DMAO. Failure of the DMAOs to act as surrogates then suggests that substrate exchange would need to be slow relative to a fast electron transfer step. In other words, after Cpd I formation in the DMAO system, the product aniline (DMA) is oxidized by one electron to form the aminium radical cation and Cpd II before any substrate exchange might occur. In contrast, the higher barrier, and thus, slower rate of electron transfer from PFDMA in the PFDMAO system could permit substrate exchange. With substrates now in competition for Cpd I, oxidative preference determines product formation. This system would be expected to demonstrate surrogacy since DMA shows lower barriers to oxidation than PFDMA (Figure 2).

Another possibility arises in the case that single electron transfer from any anilinic N-oxide is faster than substrate exchange. In this pathway, for a second substrate to be oxidized by Cpd II, a second electron transfer must occur between the aminium radical cation and the substrate to be oxidized (Scheme 9). Because the DMA radical cation has a lower formation barrier, we would expect no electron transfer from any substrates with a higher barrier to oxidation (though transfer from the isotopically distinct [^{14}C]DMA would be expected.) We would, however, expect to observe electron transfer from DMA to *p*-cyano-*N*,*N*-dimethylani-

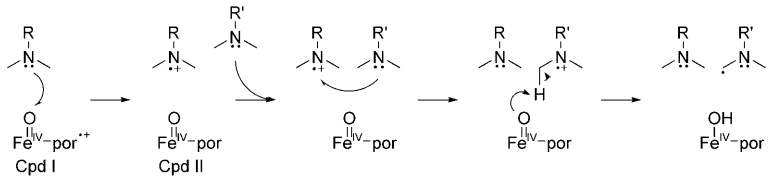

Scheme 9. Single electron transfer between two substrates of Cpd II (por = porphyrin).

line radical cation, since the electron-withdrawing nature of the *p*-cyano group would decrease its single-electron oxidation potential relative to DMA. In support of this rationale, Seto and Guengerich did see an increased support of [^{14}C]DMA oxidation by CDMAO. In the PFDMAO system, the highly electron-withdrawing nature of the aromatic fluorines poises PFDMA radical cation for accepting an electron. With PFDMA having a much lower oxidation potential, any substrate with a higher oxidation potential would be capable of transferring an electron to the PFDMA radical cation to generate a new substrate radical cation. This new radical cation would then be susceptible to oxidation by Cpd II.

The HAT and SET mechanisms predict similar outcomes for the DMAO and PFDMAO systems. In each mechanism, DMAO is not expected to support oxidation of other substrates due to the ease of DMA oxidation. Further, each mechanism also predicts the ability of PFDMAO to act as a surrogate owing to a more difficult oxidation of the product aniline (PFDMA). With DMAO seemingly unable to support oxidation of other substrates and PFDMAO supporting oxidation of DMA and CPMA, none of these mechanisms is excluded.

To distinguish between these mechanisms, we used the chemical probes of Schaffer et al. and tested the metabolism of CPMA in the PFDMAO system. Schaffer et al. found that the metabolism of CPMA distinguished between SET and HAT mechanisms.[11,12] With HRP, which follows a SET mechanism, CPMA metabolism led exclusively to cyclopropyl ring-opened products (Scheme 10). In P450, now considered to follow a HAT mechanism, strictly ring-closed products were formed (Scheme 11). We presented CPMA to the PFDMAO system and successfully observed metabolites of CPMA. Though metabolism of CPMA was much slower than that of DMA, the two products, MA and *N*-cyclopropylaniline (CPA), were observed. No ring-opened products were observed in these experiments. Being a product of both pathways, MA formation does not distinguish between HAT and SET, however, the observation of PFDMAO-supported formation of CPA, a ring-intact product, is revealing. Ring-intact product formation strongly argues against a SET mechanism in the PFDMAO system, excluding both proposed SET mechanisms. In the exclusion of SET, a HAT mechanism for N-dealkylation in the N-oxide system is supported, similar to the native P450 system.

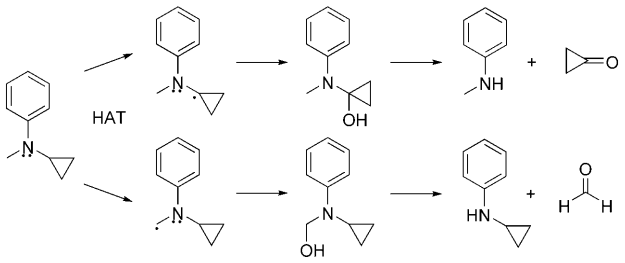

Scheme 11. Product formations from CPMA directed by a HAT mechanism.

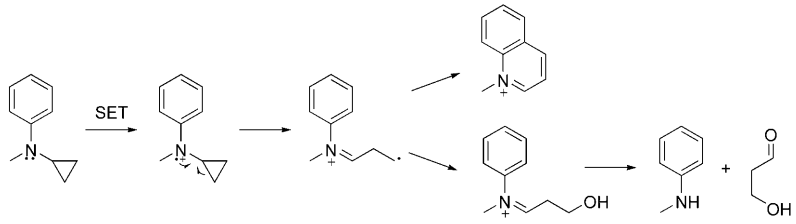

Scheme 10. Product formations from *N*-cyclopropyl-*N*-methylaniline (CPMA) directed by a SET mechanism.

To further evaluate the similarity between the anilinic N-oxide and native P450 systems, KIEs were measured for the PFDMAO–P450cam system (Table 1). In the competitive and noncompetitive intermolecular experiments, the intrinsic isotope effect is completely masked. However, the intramolecular experiment shows a significant isotope effect with a value similar to those seen for N-dealkylation by both the DMAO- and NADPH/O_2-supported systems.

KIEs were also evaluated for the N-dealkylation of DMA by the PFDMAO system (Table 4). In the noncompetitive intermolecular experiment, the intrinsic isotope effect is completely masked. However, partial unmasking of the intrinsic isotope effect is observed in the competitive experiment. This is likely due to a slow but significant exchange of the DMA prior to N-dealkylation. This permits the heme-centered oxidant to select between the two isotopically-distinct DMAs and, thus, unmask the isotope effect. That the intrinsic isotope effect is not fully unmasked suggests that this exchange is not exceedingly rapid relative to the rate of N-dealkylation. The intramolecular isotope effect showed further unmasking of the intrinsic isotope effect. As with the PFDMAO intramolecular isotope effect, this value is similar to those seen for N-dealkylation by both the DMAO- and NADPH/O_2-supported systems.

Table 4. Product isotope effects for the N-demethylation of DMA[a] by PFDMAO and P450cam.

k_H/k_D—DMA/[D_6]DMA noncompetitive[b]	k_H/k_D—DMA/[D_6]DMA competitive	k_H/k_D—DMA/[D_3]DMA intramolecular[c]
1.3 ± 0.3	1.9 ± 0.2	2.8 ± 0.2

[a] DMA = *N*,*N*-dimethylaniline. [b] [D_6]DMA = *N*,*N*-bis(trideuteriomethyl)aniline. [c] [D_3]DMA = *N*-methyl-*N*-trideuteriomethylaniline.

Studies have shown large intramolecular isotope effects (2.93–13.3) for N-dealkylation of DMAs by HRP[16,26] in contrast to the smaller isotope effects (1.40–3.87) seen by P450.[16,19,27] As HRP follows a SET mechanism, the small magnitude of the intramolecular isotope effects in the PFDMAO system further support a mechanism that does not involve single electron transfer.

As we have shown, product formation rates of DMAO and PFDMAO exclude direct Cpd II formation. Indirect formation of Cpd II derived from electron transfer to Cpd I a SET mechanism, is, in turn, excluded by the formation of CPA. In the exclusion of Cpd II-derived mechanisms, HAT is left to be the likely mechanism for N-dealkylation by the anilinic N-oxide-supported P450. Further, the similarities in KIEs for both the N-oxide and NADPH/O_2 systems, together with the observation of cyclopropyl ring-intact products in both systems, strongly support a HAT mechanism for N-dealkylation in these systems.

Conclusion

In conclusion, we have identified an N-oxide capable of supporting N-demethylation of *N*,*N*-dimethylaniline (DMA) by P450cam, implicating the generation of a porphyrin-directed reactive oxygen species (ROS) as an intermediate to oxidation. Kinetic isotope effects and product formation rates, supported by DFT calculations, support a mechanism for surrogacy that begins with a rate-determining oxene donation to form Compound I (Cpd I). Further, the formation of ring-intact products from *N*-cyclopropyl-*N*-methylaniline (CPMA) support a mechanism similar to that of native P450, with the ring-intact products excluding a single electron transfer (SET) mechanism. The apparent similarities in the native and N-oxide-supported systems together with support for the formation of Cpd I argue for a Cpd I-directed hydrogen atom transfer (HAT) mechanism for P450-mediated N-demethylation similar to that proposed for P450-mediated alkyl hydroxylation. Further, these similarities demonstrate the ability of the N-oxide-generated oxidant to act as an accurate mimic of the native system, which supports the use of N-oxides as mechanistic probes for other P450-mediated oxidations. The application of anilinic N-oxides as mechanistic probes as well as their potential as oxygen surrogates for synthesis in porphyrin mimetic systems are currently under investigation by our group.

Experimental Section

Materials: Reagents or HPLC grade chemicals and solvents were supplied by Alfa Aesar (Ward Hill, MA), Aldrich (St. Louis, MO), Fisher Scientific (Pittsburgh, PA), EMD (Gibbstown, NJ), and Mallinckrodt Baker (Phillipsburg, NJ). Isotopically-labeled compounds were supplied by CDN Isotopes (Pointe-Claire, Quebec, CA). THF was distilled under argon from sodium and benzophenone prior to use. ^{1}H NMR spectra were obtained at 300 MHz with a Varian Mercury 300 spectrometer equipped with a quad-detection probe (^{1}H, ^{13}C, ^{31}P, and ^{19}F). ^{1}H-decoupled ^{13}C NMR spectra were obtained at 75 MHz. ^{19}F NMR spectra were obtained at 282 MHz. Gas chromatography/mass spectrometry was performed on a ThermoQuest Voyager GC/MS (Thermo-Finnegan) coupled to a CE Instruments GC8000Top affixed with a 30 m JW Scientific DB-1 GC column. Liquid chromatography/mass spectrometry was performed on a ThermoQuest Surveyor LC affixed with an Agilent Eclipse Plus C-18 column (5 μm, 2.1 × 150 mm) coupled to a Thermo-Finnegan LCQ Advantage ESI-MS.

N-Oxide-supported P450cam—general procedure: P450cam was expressed and purified as described previously.[28] Incubations of P450cam with 2,3,4,5,6-pentafluoro-*N*,*N*-dimethylaniline *N*-oxide (PFDMAO) or *N*,*N*-dimethylaniline *N*-oxide (DMAO) were performed by using N-oxide and P450cam in phosphate buffer (100 mM, pH 7.4). Samples were preincubated at 30 °C prior to initiation with the N-oxide. For rate determinations, reactions were incubated at 30 °C for discrete time points up to 60 min, dependent on the reaction. Reactions were quenched with ethyl acetate containing 2,3,4,5,6-pentafluoroaniline (PFA) as an internal standard. The organic layer was collected and product further extracted twice with ethyl acetate. Extracts were combined, dried with $MgSO_4$, and concentrated in a 35 °C bath under a flow of $N_{2(g)}$ to < 300 μL. Reaction products were monitored by gas chromatography–mass spectrometry (GC–MS) by using electron impact ionization. Except where indicated, the GC method began at 70 °C for 5 min followed first by a 10 °C min^{-1} ramp to 120 °C then by a 30 °C min^{-1} ramp to 230 °C.

DMAO-supported P450cam procedure: Following the general procedure above, incubations were performed by using DMAO hydrochloride (20 μmol) and P450cam (1.0 nmol) in phosphate buffer (1.0 mL, 100 mM, pH 7.4). Samples were preincubated at 30 °C for 10 min prior to initiation with the N-oxide. For rate determinations, reactions were incubated at 30 °C and quenched at time points 0, 10, 20, 30, 45, and 60 min with ethyl acetate (500 μL) containing PFA (50 nmol) as an internal standard. Additional ethyl acetate (500 μL) was added for product extraction. Product was further extracted with ethyl acetate (2 × 1.0 mL). Extracts were combined, dried with $MgSO_4$, and concentrated in a 35 °C bath under a flow of $N_{2(g)}$ to < 300 μL. Reaction products were monitored by GC–MS using electron impact ionization with the general method described above. Ions with *m*/*z* 107.1 were monitored for quantization of *N*-methylaniline (MA).

PFDMAO-supported P450cam procedure: Following the general procedure above, incubations were performed by using the trifluoroacetic acid salt of PFDMAO (13 μmol) and P450cam (1.0 nmol) in phosphate buffer (1.0 mL, 100 mM, pH 7.4). Samples were preincubated at 30 °C for 10 min prior to initiation with the N-oxide. For rate determinations, reactions were incubated at 30 °C for discrete time points up to and including 60 min. Reactions were quenched with ethyl acetate (500 μL) containing PFA (50 nmol) as an internal standard. Additional ethyl acetate (500 μL) was added for product extraction. Product was further extracted with ethyl acetate (2 × 1.0 mL). Extracts were combined, dried with $MgSO_4$, and concentrated in a 35 °C bath under a flow of $N_{2(g)}$ to < 300 μL. Reaction products were monitored by GC–MS by using electron impact ionization with the general method described above. Ions with *m*/*z* 193.1 and 211.1 were monitored for quantization of 2,3,4,5,6-pentafluoro-*N*-methylaniline (PFMA) and 2,3,4,5,6-pentafluoro-*N*,*N*-dimethylaniline (PFDMA), respectively.

PFDMAO surrogacy procedure: Following the PFDMAO-supported incubation procedure above, incubations were performed by using samples consisting of the trifluoroacetic acid salt of PFDMAO (13 μmol), P450cam (1.0 nmol), and *N*,*N*-dimethylaniline (DMA) or *N*-cyclopropyl-

N-methylaniline (CPMA) (20 μmol) in phosphate buffer (1.0 mL, 100 mM, pH 7.4). GC–MS was performed by using the general method above monitoring ions with *m*/*z* 107.1, 132.1, 193.1, and 211.1 for MA, *N*-cyclopropylaniline (CPA), PFMA, and PFDMA, respectively.

PFDMAO intermolecular kinetic isotope effect (KIE) determinations: Samples consisted of the trifluoroacetic acid salt of PFDMAO (1.3 μmol) and/or 2,3,4,5,6-pentafluoro-*N*,*N*-bis(trideuteriomethyl)aniline *N*-oxide ([D_6]PFDMA) (1.3 μmol), and P450cam (1.0 nmol) in phosphate buffer (1.0 mL, 100 mM, pH 7.4). Samples were preincubated at 30 °C for 5.0 min. Reactions were initiated by addition of N-oxide and incubated at 30 °C for 60 min. Reactions were quenched with dichloromethane (1.0 mL) and anisole (20 nmol) in dichloromethane (100 μL) was added as an internal standard. The organic layer was collected and product further extracted with dichloromethane (2×1.0 mL). Extracts were combined, dried with $MgSO_4$, and concentrated in a 35 °C bath under a flow of $N_{2(g)}$ to <300 μL. Reaction products were monitored by GC–MS by using electron impact ionization with the following method. The GC method began at 35 °C for 5 min followed by a 20 °C min^{-1} ramp to 230 °C. Ions with *m*/*z* 197.1 and 200.1 were monitored for quantization of PFMA and 2,3,4,5,6-pentafluoro-*N*-trideuteriomethylaniline ([D_3]PFMA), respectively.

PFDMAO intramolecular KIE determination: Following the general incubation procedure above, samples consisted of the trifluoroacetic acid salt of 2,3,4,5,6-pentafluoro-*N*-methyl-*N*-(trideuteriomethyl)aniline *N*-oxide ([D_3]PFDMA) (670 nmol) and P450cam (1.0 nmol). Samples were preincubated at 30 °C for 5.0 min. Reactions were initiated by addition of N-oxide and incubated at 30 °C for 20 min. Reactions were quenched with PFA (50 nmol) in ethyl acetate (500 μL). Additional ethyl acetate (500 μL) was added for product extraction. Product was further extracted with ethyl acetate (2×1.0 mL). Extracts were combined, dried with $MgSO_4$, and concentrated in a 35 °C bath under a flow of $N_{2(g)}$ to <300 μL. Reaction products were monitored by GC–MS by using electron impact ionization with the general method described above. 3 Da spans of ions with *m*/*z* 194.6–197.6 and 197.6–200.6 were monitored for quantization of PFMA and [D_3]PFMA, respectively, correcting for isotopic overlap.

DMA KIE determinations: Following the general incubation procedure, samples consisted of the trifluoroacetate salt of PFDMAO (670 nmol), P450cam (1.0 nmol), and the appropriate DMA. Noncompetitive reactions used either DMA (1.0 μmol) or *N*,*N*-bis(trideuteriomethyl)aniline ([D_6]DMA) (1.0 μmol). Competitive reactions contained both DMA (1.0 μmol) and [D_6]DMA (1.0 μmol). Intramolecular experiments contained *N*-methyl-*N*-trideuteriomethylaniline ([D_3]DMA) (1.0 μmol). Samples were preincubated at 30 °C for 8.0 min. Reactions were initiated by addition of PFDMAO and incubated for 20 min at 30 °C. Reactions were quenched with PFA (20 nmol) in ethyl acetate (500 μL). Additional ethyl acetate (500 μL) was added for product extraction. Product was further extracted with ethyl acetate (2×1.0 mL). Extracts were combined, dried with $MgSO_4$. Reaction products were monitored without concentration by GC–MS by using electron impact ionization with the general method described above. For the noncompetitive assays, 4 Da spans of ions with *m*/*z* 105.6–109.6 and 107.6–111.6 were monitored for quantization of MA and *N*-trideuteriomethylaniline ([D_3]MA), respectively. For the competitive and intramolecular assays, 3 Da spans of ions with *m*/*z* 104.6–107.6, 107.6–110.6 were monitored correcting for isotopic overlap.

***p*-Cyano-*N*,*N*-dimethylaniline *N*-oxide (CDMAO) intermolecular KIE determinations**: Samples containing CDMAO (1.0 μmol) and/or *p*-cyano-*N*,*N*-bis(trideuteriomethyl)aniline *N*-oxide ([D_6]CDMAO) (1.0 μmol) and P450cam (5 nmol) in phosphate buffer (500 μL, 100 mM, pH 7.4) were incubated for 60 min at 30 °C. Reactions were quenched with acetonitrile (1.0 mL) containing aniline (30 nmol) as an internal standard followed by vortexing and centrifugation to pellet the protein. Supernatant was collected and reaction products monitored by LC–ESIMS. The LC method began at 5% methanol, 0.1% acetic acid in water for 2.0 min followed by a 5% methanol min^{-1} ramp to 95% methanol, 0.1% acetic acid in water (2.0–20.0 min). Ions with *m*/*z* 133.1 and 136.1 were monitored for *p*-cyano-*N*-methylaniline (CMA) and *p*-cyano-*N*-trideuteriomethylaniline ([D_3]CMA), respectively.

***p*-Cyano-*N*,*N*-dimethylaniline *N*-oxide hydrate**: *m*-Chloroperbenzoic acid (75%, 250 mg, 1.1 mmol) in chloroform (1.8 mL) was added dropwise to a stirring solution of *p*-cyano-*N*,*N*-dimethylaniline (146 mg, 1.0 mmol) in chloroform (2 mL). The reaction was allowed to proceed for 3.0 h on ice. The product was purified by chromatography by using basic alumina. The product mixture was loaded with chloroform and eluted with 25% methanol in chloroform. Solvents were removed by rotary evaporation to yield a white solid (178 mg, 99%). ^{1}H NMR (300 MHz, $CDCl_3$): δ=2.83 (br s, 2H), 3.62 (s, 6H), 7.82 (d, J=7.2 Hz, 2H), 8.17 ppm (d, J=6.9 Hz, 2H); ^{13}C{^{1}H} NMR (75 MHz, $CDCl_3$): δ=63.49, 113.70, 117.70, 121.61, 133.58, 158.02 ppm.

***N*,*N*-Dimethylaniline *N*-oxide hydrochloride**: DMA (1.27 mL, 10 mmol) was added dropwise to a mixture of *m*-chloroperbenzoic acid (75%, 3.45 g, 15 mmol) in dichloromethane (35 mL). Reaction was run for 1.5 h at room temperature and the solvent was removed by rotary evaporation. The product mixture was purified by column chromatographed by using basic alumina. The product was loaded with chloroform and eluted with 25% methanol in chloroform. Fractions containing product were combined and the solvent was removed by rotary evaporation. The product was reconstituted with water (10 mL) and the solution was rinsed with diethyl ether (2×10 mL). Water was removed by rotary evaporation to give oil. Concentrated hydrochloric acid (1 mL) was added to the oil and the mixture was concentrated in vacuum to give a solid. The product was recrystallized from acetone to yield long, colorless crystals (350 mg, 20%). ^{1}H NMR (300 MHz, $CDCl_3$): δ=4.09 (s, 6H), 7.55 (m, 3H), 7.91 (d, J=8.4 Hz, 2H), 13.86 ppm (br s, 1H); ^{13}C{^{1}H} NMR (75 MHz, $CDCl_3$): δ=61.06, 119.56, 130.48, 131.20, 149.03 ppm.

2,3,4,5,6-Pentafluoro-*N*-methylaniline: Potassium *tert*-butoxide (*t*BuOK) (2.0 g, 18 mmol) was added at room temperature over 2 min to a vigorously stirring solution of 2,3,4,5,6-pentafluoroaniline (2.8 g, 15 mmol) and iodomethane (0.94 mL, 15 mmol) in dry THF (100 mL). TLC after addition of potassium *tert*-butoxide showed incomplete conversion of the starting material with a trace of doubly methylated product present. Precipitates (potassium iodide and unreacted *t*BuOK) were removed by filtration through Celite. THF was removed from the filtrate by rotary evaporation to a volume of 5 mL. The mixture was then purified by column chromatography over Silica 60, eluting the product with 2.5% ethyl acetate in hexane to give 2,3,4,5,6-pentafluoro-*N*-methyl aniline (1.27 g, 43%) as a pale yellow oil. ^{1}H NMR (300 MHz, $CDCl_3$): δ=3.05 (m, 3H), 3.58 ppm (br s, 1H); ^{13}C{^{1}H} NMR (75 MHz, $CDCl_3$): δ=33.60 ppm; ^{19}F NMR (282 MHz, $CDCl_3$): δ=−172.84 (m, 1F), −165.13 (m, 2F), −161.13 ppm (d, J=23.7 Hz, 2F).

2,3,4,5,6-Pentafluoro-*N*,*N*-dimethylaniline: *t*BuOK (5.0 g, 45 mmol) was added at room temperature over 10 min to a vigorously stirring solution of 2,3,4,5,6-pentafluoroaniline (2.8 g, 15 mmol) and iodomethane (2.3 mL, 38 mmol) in dry THF (100 mL). TLC after 10 min showed complete conversion of the starting material to 2,3,4,5,6-pentafluoro-*N*,*N*-dimethylaniline. Precipitates (potassium iodide and unreacted *t*BuOK) were removed by filtration through Celite. THF was removed from the filtrate by rotary evaporation to a volume of 5 mL. The product was purified by flash chromatography (15% chloroform in hexane) to yield 2,3,4,5,6-pentafluoro-*N*,*N*-dimethylaniline (1.68 g, 53%) as a clear oil. ^{1}H NMR (300 MHz, $CDCl_3$): δ=2.90 ppm (t, J=1.8 Hz, 6H); ^{13}C{^{1}H} NMR (75 MHz, $CDCl_3$): δ=43.71 ppm (t, J=3.6 Hz); ^{19}F NMR (282 MHz, $CDCl_3$): δ=−165.19 (t, J=21.7 Hz, 1F), −164.53 (m, 2F), −151.25 ppm (d, J=21.7 Hz, 2F).

2,3,4,5,6-Pentafluoro-*N*,*N*-dimethylaniline *N*-oxide trifluoroacetic acid salt: *t*BuOK (16.8 g, 150 mmol) was added at room temperature over 5 min to a vigorously stirring solution of 2,3,4,5,6-pentafluoroaniline (9.16 g, 50 mmol) and iodomethane (7.8 mL, 125 mmol) in dry THF (200 mL). TLC after 10 min showed complete conversion of the starting material to 2,3,4,5,6-pentafluoro-*N*,*N*-dimethylaniline. Precipitates (potassium iodide and unreacted *t*BuOK) were removed by filtration through Celite. THF was distilled from the filtered product mixture and the product was dissolved in dichloromethane (50 mL) and stirred on ice. Trifluoroperacetic acid (TFPA) was generated in situ by using a method adapted from Emmons and Lucas.[29] Hydrogen peroxide (50%, 7.1 mL, 125 mmol) was added dropwise to dichloromethane (12 mL) stirring on

ice. To this mixture, trifluoroacetic anhydride (21.1 mL, 150 mmol) was added dropwise over 20 min. After stirring the reaction for 20 min, the mixture was warmed to room temperature. The TFPA mixture was added dropwise over 15 min to the stirring PFDMA mixture on ice. TLC after 120 min showed only a trace of PFDMA in the reaction mixture. The product was extracted from the reaction mixture with distilled water (7×50 mL). Extracts were combined and rinsed with diethyl ether (100 mL). Water was removed by rotary evaporation and the product was precipitated with diethyl ether. The product was then recrystallized from diethyl ether/THF (75:25) to yield 2,3,4,5,6-pentafluoro-*N*,*N*-dimethylaniline *N*-oxide trifluoroacetic acid salt (6.36 g, 37%) as large pale yellow crystals. ^{1}H NMR (300 MHz, $CDCl_3$): δ=4.14 (t, J=1.8 Hz, 6H), 11.20 ppm (brs, 1H); ^{13}C{^{1}H} NMR (75 MHz, $CDCl_3$): δ=62.6 ppm (t, J=5.7 Hz,); ^{19}F NMR (282 MHz, $CDCl_3$): δ=−156.95 (m, 2F), −146.99 (m, 1F), −138.32 (d, J=17.8 Hz, 2F), −76.46 ppm (s, 3F).

***N*-Cyclopropyl-*N*-methylaniline**: *N*-Cyclopropyl-*N*-methylaniline was synthesized by using the method of Shaffer et al.[11] Ethylmagnesium bromide (3.0 M in Et_2O, 10 mL, 30 mmol) was added dropwise to a stirring solution of *N*-methylformanilide (1.3 mL, 10 mmol) and titanium isopropoxide (3.8 mL, 14 mmol) in dry THF (50 mL). The reaction was heated at 65°C for 30 min followed by stirring for 24 h at room temperature. The reaction was quenched with a saturated aqueous solution of NH_4Cl (40 mL) and THF was removed by rotary evaporation. The product mixture was diluted with 1N HCl (36 mL) and the product was extracted with diethyl ether (7×13 mL). The combined extracts were dried with $MgSO_4$, filtered through Celite, and the solvent was removed by rotary evaporation to give oil. The product was purified by flash chromatography (15% CH_2Cl_2 in hexane) to yield *N*-cyclopropyl-*N*-methylaniline (590 mg, 40%) as a pale yellow oil. ^{1}H NMR (300 MHz, $CDCl_3$): δ=0.64 (m, 2H), 0.84 (m, 2H), 2.39 (m, 1H), 3.00 (s, 3H), 6.79 (t, J=7.5 Hz, 1H), 7.01 (d, J=7.5 Hz, 2H), 7.27 ppm (t, J=7.5 Hz, 2H); ^{13}C{^{1}H} NMR (75 MHz, $CDCl_3$): δ=9.31, 33.52, 39.34, 114.01, 117.62, 129.07, 151.10 ppm.

***N*-(1-Ethoxycyclopropyl)aniline**: *N*-(1-Ethoxycyclopropyl)aniline was synthesized from aniline and 1-ethoxy-1-bromocyclopropane by using the methods of Kang and Kim[30] and Leoppky and Elomari.[31] 1-Ethoxy-1-bromocyclopropane was generated in situ by using the methods of Gadwood et al.[32] Phosphorous tribromide (375 μL, 4.0 mmol) was directly added dropwise to 1-ethoxy-1-trimethylsiloxycyclopropane (1.0 mL, 5.0 mmol) while stirring on ice. After addition, the reaction was removed from ice and stirred for 7 h at room temperature. The completion of the reaction was shown by ^{1}H NMR spectroscopy. The reaction mixture was brought up in pentane (5 mL) and placed in an acetone/dry ice bath (−25°C). While stirring, a saturated aqueous solution of Na_2CO_3 (2.5 mL) was added dropwise over 3 min and the organic layer was collected. The aqueous layer was washed with pentane (2×2 mL). The combined organic layers were dried with Na_2SO_4 and filtered under vacuum to a final volume of 1 mL. The filtrate was added dropwise to a stirring solution of aniline (370 μL, 4.0 mmol) and triethylamine (700 μL, 5.0 mmol) in pentane (1.5 mL) and the reaction mixture was heated to reflux for 72 h. The reaction mixture was brought up in dichloromethane (15 mL) and washed with distilled water (2×10 mL) and with saturated brine (10 mL). The aqueous layers were combined and back-extracted with dichloromethane (15 mL). The two organic layers were combined and the solvent was removed by rotary evaporation. The product was purified by flash chromatography (10% ethyl acetate in hexane) to yield *N*-(1-ethoxycyclopropyl)aniline (273 mg, 39%) as a pale yellow oil. ^{1}H NMR (300 MHz, $CDCl_3$): δ=0.89 (q, J=4.5 Hz, 2H), 1.13 (m, 5H), 3.57 (q, J=7.2 Hz, 2H), 4.79 (brs, 1H), 6.77 (t, J=7.5 Hz, 1H), 6.88 (d, J=7.2 Hz, 2H), 7.20 ppm (t, J=7.5 Hz, 2H); ^{13}C{^{1}H} NMR (75 MHz, $CDCl_3$): δ=15.23, 15.58, 61.11, 68.77, 114.36, 118.57, 129.27, 145.71 ppm.

***N*-Cyclopropylaniline**: *N*-Cyclopropylaniline was synthesized from *N*-(1-ethoxycyclopropyl)aniline by using the methods of Kang and Kim[30] and Leoppky and Elomari.[31] Boron trifluoride etherate (390 μL, 3.1 mmol) was added dropwise to a stirring suspension of sodium borohydride (117 mg, 3.1 mmol) in THF (3.0 mL) on ice under an argon atmosphere and the mixture was stirred for 30 min. *N*-(1-Ethoxycyclopropyl)aniline (270 mg, 1.5 mmol) was added dropwise to the stirring mixture on ice. The reaction mixture was removed from ice and stirred for 12 h allowing to warm to room temperature. The reaction was carefully quenched with distilled water (10 drops) and brought up in diethyl ether (10 mL). The mixture was washed with distilled water (3×5 mL) and with brine (5 mL). The organic layer was dried with Na_2SO_4, filtered and, the solvent was removed by rotary evaporation. The product was purified by flash chromatography (4% ethyl acetate in hexane) to yield *N*-cyclopropylaniline (125 mg, 61%) as a pale yellow oil. ^{1}H NMR (300 MHz, $CDCl_3$): δ=0.44 (m, 2H), 0.65 (m, 2H), 2.35 (m, 1H), 4.09 (brs, 1H), 6.67 (t, J=7.2 Hz, 1H), 6.72 (d, J=7.5 Hz, 2H), 7.12 ppm (t, J=7.2 Hz, 2H); ^{13}C{^{1}H} NMR (75 MHz, $CDCl_3$): δ=7.63, 25.45, 113.37, 117.95, 129.34, 148.90 ppm.

Computational methods: Density functional calculations were performed by using Gaussian 03[33] or Jaguar[34]. The B3LYP[24] functional was used with the LACVP basis set with effective core potential on iron and the 6-31G on sulfur, nitrogen, carbon, and hydrogen. Energies are reported as enthalpies of gas-phase reactions without correction for zero-point energies or solvation effects. The optimized geometries are available in the Supporting Information. The heme model was the abbreviated heme with an S−H as fifth ligand used by Shaik and co-workers.[17] The spin density was calculated for the ground state radical cation by using standard Mulliken population analysis.

Acknowledgements

This work was supported by NIH Grant GM84546.

[1] P. R. Ortiz de Montellano, *Cytochrome P450:Structure, Mechanism, and Biochemistry*, Plenum, New York, **1995**.
[2] J. T. Groves, G. A. McClusky, R. E. White, M. J. Coon, *Biochem. Biophys. Res. Commun.* **1978**, *81*, 154–160.
[3] M. Newcomb, R. Zhang, R. E. P. Chandrasena, J. A. Halgrimson, J. H. Horner, T. M. Makris, S. G. Sligar, *J. Am. Chem. Soc.* **2006**, *128*, 4580–4581.
[4] G. M. Raner, J. I. Thompson, A. Haddy, V. Tangham, N. Bynum, G. Ramachandra Reddy, D. P. Ballou, J. H. Dawson, *J. Inorg. Biochem.* **2006**, *100*, 2045–2053.
[5] P. R. Ortiz de Montellano, J. J. De Voss, *Nat. Prod. Rep.* **2002**, *19*, 477–493.
[6] Y. Wang, D. Kumar, C. Yang, K. Han, S. Shaik, *J. Phys. Chem. B* **2007**, *111*, 7700–7710.
[7] J. Shearer, C. X. Zhang, L. Q. Hatcher, K. D. Karlin, *J. Am. Chem. Soc.* **2003**, *125*, 12670–12671.
[8] J. Shearer, C. X. Zhang, L. N. Zakharov, A. L. Rheingold, K. D. Karlin, *J. Am. Chem. Soc.* **2005**, *127*, 5469–5483.
[9] P. Comba, S. Kuwata, G. Linti, H. Pritzkow, M. Tarnai, H. Wadepohl, *Chem. Commun.* **2006**, 2074–2076.
[10] K. Nehru, M. S. Seo, J. Kim, W. Nam, *Inorg. Chem.* **2007**, *46*, 293–298.
[11] C. L. Shaffer, M. D. Morton, R. P. Hanzlik, *J. Am. Chem. Soc.* **2001**, *123*, 8502–8508.
[12] C. L. Shaffer, S. Harriman, Y. M. Koen, R. P. Hanzlik, *J. Am. Chem. Soc.* **2002**, *124*, 8268–8274.
[13] F. P. Guengerich, O. Okazaki, Y. Seto, T. L. Macdonald, *Xenobiotica* **1995**, *25*, 689–709.
[14] Y. Goto, Y. Watanabe, S. Fukuzumi, J. P. Jones, J. P. Dinnocenzo, *J. Am. Chem. Soc.* **1998**, *120*, 10762–10763.
[15] M. A. Cerny, R. P. Hanzlik, *J. Am. Chem. Soc.* **2006**, *128*, 3346–3354.
[16] F. P. Guengerich, C.-H. Yun, T. L. MacDonald, *J. Biol. Chem.* **1996**, *271*, 27321–27329.
[17] K. Y. Cho, Y. Moreau, D. Kumar, D. A. Rock, J. P. Jones, S. Shaik, *Chem. Eur. J.* **2007**, *13*, 4103–4115.
[18] N. Bichara, M. S. Ching, C. L. Blake, H. Ghabrial, R. A. Smallwood, *Drug Metab. Dispos.* **1996**, *24*, 112–118.

[19] T. S. Dowers, D. A. Rock, D. A. Rock, J. P. Jones, *J. Am. Chem. Soc.* **2004**, *126*, 8868–8869.
[20] M. W. Nee, T. C. Bruice, *J. Am. Chem. Soc.* **1982**, *104*, 6123–6125.
[21] Y. Seto, F. P. Guengerich, *J. Biol. Chem.* **1993**, *268*, 9986–9997.
[22] J. T. Pearson, J. J. Hill, J. Swank, N. Isoherranen, K. L. Kunze, W. M. Atkins, *Biochemistry* **2006**, *45*, 6341–6353.
[23] C. Li, W. Wu, K.-B. Cho, S. Shaik, *Chem. Eur. J.* **2009**, *15*, 8492–8503.
[24] A. D. Becke, *J. Chem. Phys.* **1993**, *98*, 5648–5652.
[25] Q. Wang, X. Sheng, J. H. Horner, M. Newcomb, *J. Am. Chem. Soc.* **2009**, *131*, 10629–10636.
[26] O. Okazaki, F. P. Guengerich, *J. Biol. Chem.* **1993**, *268*, 1546–1552.
[27] J. P. Dinnocenzo, S. B. Karki, J. P. Jones, *J. Am. Chem. Soc.* **1993**, *115*, 7111–7116.
[28] K. J. French, M. D. Strickler, D. A. Rock, D. A. Rock, G. A. Bennett, J. L. Wahlstrom, B. M. Goldstein, J. P. Jones, *Biochemistry* **2001**, *40*, 9532–9538.
[29] W. D. Emmons, G. B. Lucas, *J. Am. Chem. Soc.* **1955**, *77*, 2287–2288.
[30] J. Kang, K. S. Kim, *J. Chem. Soc. Chem. Commun.* **1987**, 897–898.
[31] R. N. Loeppky, S. Elomari, *J. Org. Chem.* **2000**, *65*, 96–103.
[32] R. C. Gadwood, M. R. Rubino, S. C. Nagarajan, S. T. Michel, *J. Org. Chem.* **2002**, *67*, 3255–3260.
[33] Gaussian 03, Revision C.02, M. J. T. Frisch, G. W. Schlegel, H. B. Scuseria, G. E. Robb, M. A. Cheeseman, J. R. Montgomery, Jr., J. A. Vreven, T. Kudin, K. N. Burant, J. C. Millam, J. M. Iyengar, S. S. Tomasi, J. Barone, V. Mennucci, B. Cossi, M. Scalmani, G. Rega, N. Petersson, G. A. Nakatsuji, H. Hada, M. Ehara, M. Toyota, K. Fukuda, R. Hasegawa, J. Ishida, M. Nakajima, T. Honda, Y. Kitao, O. Nakai, H. Klene, M. Li, X. Knox, J. E. Hratchian, H. P. Cross, J. B. Bakken, V. Adamo, C. Jaramillo, J. Gomperts, R. Stratmann, R. E. Yazyev, O. Austin, A. J. Cammi, R. Pomelli, C. Ochterski, J. W. Ayala, P. Y. Morokuma, K. Voth, G. A. Salvador, P. Dannenberg, J. J. Zakrzewski, V. G. Dapprich, S. Daniels, A. D. Strain, M. C. Farkas, O. Malick, D. K. Rabuck, A. D. Raghavachari, K. Foresman, J. B. Ortiz, J. V. Cui, Q. Baboul, A. G. Clifford, S. Cioslowski, J. Stefanov, B. B. Liu, G. Liashenko, A. Piskorz, P. Komaromi, I. Martin, R. L. Fox, D. J. Keith, T. Al-Laham, M. A. Peng, C. Y. Nanayakkara, A. Challacombe, M. Gill, P. M. W. Johnson, B. Chen, W. Wong, M. W. C. Gonzalez, J. A Pople, Gaussian, Inc, Wallingford CT, **2004**.
[34] Jaguar, Schrodinger, Portland, OR (USA), 2006.

Received: January 23, 2010
Published online: June 2, 2010

